Bi-allelic Variants in *IQSEC1* Cause Intellectual Disability, Developmental Delay, and Short Stature

Muhammad Ansar,[1,21] Hyung-lok Chung,[2,3,18,21] Ali Al-Otaibi,[4] Mohammad Nael Elagabani,[5,6] Thomas A. Ravenscroft,[2,3] Sohail A. Paracha,[7] Ralf Scholz,[8] Tayseer Abdel Magid,[4] Muhammad T. Sarwar,[7] Sayyed Fahim Shah,[9] Azhar Ali Qaisar,[10] Periklis Makrythanasis,[1,11] Paul C. Marcogliese,[2,3] Erik-Jan Kamsteeg,[12] Emilie Falconnet,[1] Emmanuelle Ranza,[1,13,14] Federico A. Santoni,[1,15] Hesham Aldhalaan,[16] Ali Al-Asmari,[17] Eissa Ali Faqeih,[17] Jawad Ahmed,[7] Hans-Christian Kornau,[5,8] Hugo J. Bellen,[2,3,18,19,*] and Stylianos E. Antonarakis[1,13,20,*]

We report two consanguineous families with probands that exhibit intellectual disability, developmental delay, short stature, aphasia, and hypotonia in which homozygous non-synonymous variants were identified in *IQSEC1* (GenBank: NM_001134382.3). In a Pakistani family, the *IQSEC1* segregating variant is c.1028C>T (p.Thr343Met), while in a Saudi Arabian family the variant is c.962G>A (p.Arg321Gln). *IQSEC1-3* encode guanine nucleotide exchange factors for the small GTPase ARF6 and their loss affects a variety of actin-dependent cellular processes, including AMPA receptor trafficking at synapses. The ortholog of *IQSEC*s in the fly is *schizo* and its loss affects growth cone guidance at the midline in the CNS, also an actin-dependent process. Overexpression of the reference *IQSEC1* cDNA in wild-type flies is lethal, but overexpression of the two variant *IQSEC1* cDNAs did not affect viability. Loss of *schizo* caused embryonic lethality that could be rescued to 2nd instar larvae by moderate expression of the human reference cDNA. However, the p.Arg321Gln and p.Thr343Met variants failed to rescue embryonic lethality. These data indicate that the variants behave as loss-of-function mutations. We also show that *schizo* in photoreceptors is required for phototransduction. Finally, mice with a conditional *Iqsec1* deletion in cortical neurons exhibited an increased density of dendritic spines with an immature morphology. The phenotypic similarity of the affecteds and the functional experiments in flies and mice indicate that *IQSEC1* variants are the cause of a recessive disease with intellectual disability, developmental delay, and short stature, and that axonal guidance and dendritic projection defects as well as dendritic spine dysgenesis may underlie disease pathogenesis.

Introduction

Much progress has been made in the past few years in the identification of genes responsible for intellectual disabilities (ID), yet more than half of all cases remain undiagnosed.[1,2] It has been estimated that the total number of genes involved in autosomal-recessive ID could be in the thousands.[1,3,4] Autosomal-recessive disorders are common in consanguineous populations[5–7] and we have therefore focused on studying consanguineous families with more than a single affected sibling to identify recessive genes that cause ID and improve genetic diagnosis.[7]

Here, we present compelling data that *IQSEC1* (MIM: 610166) is the cause of a syndrome with ID. *IQSEC1* is part of a family of three genes. The ortholog in flies,[8] *schizo*, was shown to affect axon guidance[9] and myoblast fusion.[10,11] IQSEC1, 2, 3 and Schizo all have an IQ-like motif and a Sec7-PH tandem domain. They are members of a family of guanine nucleotide exchange factors (GEFs) for ARF family GTPases and have been shown to regulate endosomal trafficking and actin cytoskeletal remodeling. IQSEC1/BRAG2 has been found in multiple tissues and is implicated in a variety of functions including myoblast fusion, integrin trafficking, angiogenesis, and cancer metastasis.[12]

In the mammalian brain, IQSEC1/BRAG2 and IQSEC2/BRAG1 are concentrated at the postsynaptic density of glutamatergic synapses.[13–16] Both proteins have been shown to control activity-dependent removal of AMPA receptors from glutamatergic synapses, a process that is required for long-term synaptic depression[15,17,18] and involved in forgetting.[19] Moreover, both proteins are sequentially recruited by NMDA receptors to activate Arf6 during neuronal development and this is crucial for the maturation of glutamatergic synapses.[20] Pathogenic

[1]Department of Genetic Medicine and Development, University of Geneva, 1211 Geneva, Switzerland; [2]Department of Molecular and Human Genetics, Baylor College of Medicine, Houston, TX 77030, USA; [3]Jan and Dan Duncan Neurological Research Institute, Texas Children's Hospital, Houston, TX 77030, USA; [4]King Fahad Medical City, National Neuroscience Institute, 12231 Riyadh, Saudi Arabia; [5]Neuroscience Research Center (NWFZ), Charité - Universitätsmedizin Berlin, 10117 Berlin, Germany; [6]Freie Universität Berlin, Department of Biology, Chemistry, and Pharmacy, 14195 Berlin, Germany; [7]Institute of Basic Medical Sciences, Khyber Medical University, 25100 Peshawar, Pakistan; [8]Center for Molecular Neurobiology (ZMNH), University of Hamburg, 20251 Hamburg, Germany; [9]Department of Medicine, KMU Institute of Medical Sciences, 26000 Kohat, Pakistan; [10]Radiology department, Lady reading Hospital, 25000 Peshawar, Pakistan; [11]Biomedical Research Foundation of the Academy of Athens, 115 27 Athens, Greece; [12]Department of Human Genetics, Radboud University Medical Center, 6525 GA Nijmegen, the Netherlands; [13]Service of Genetic Medicine, University Hospitals of Geneva, 1205 Geneva, Switzerland; [14]Current address, Medigenome, The Swiss Institute of Genomic Medicine, 1207 Geneva, Switzerland; [15]Department of Endocrinology Diabetes and Metabolism, University hospital of Lausanne, 1011 Lausanne, Switzerland; [16]King Faisal Specialist Hospital & Research Centre, 12713 Riyadh, Saudi Arabia; [17]Medical Genetics Department, Children's Hospital, King Fahad Medical City, 12231 Riyadh, Saudi Arabia; [18]Howard Hughes Medical Institute, Houston TX 77030, USA; [19]Department of Neuroscience and Program in Developmental Biology, Baylor College of Medicine, Houston, TX 77030, USA; [20]iGE3 Institute of Genetics and Genomics of Geneva, 1211 Geneva, Switzerland
[21]These authors contributed equally to this work
*Correspondence: hbellen@bcm.edu (H.J.B.), stylianos.antonarakis@unige.ch (S.E.A.)
https://doi.org/10.1016/j.ajhg.2019.09.013.

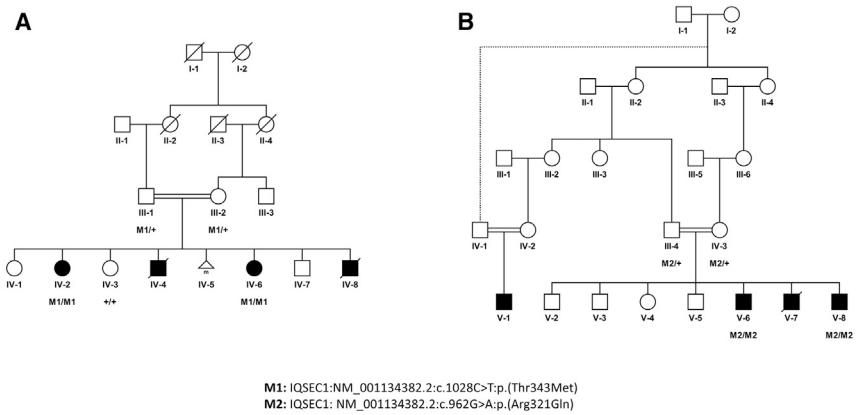

Figure 1. Segregation of *IQSEC1* Variants in Two Families with Overlapping Neurodevelopmental Phenotypes
Pedigree trees showing segregation of rare homozygous pathogenic *IQSEC1* variants c.1028C>T (p.Thr343Met) in family 1 (A) and c.962G>A (p.Arg321Gln) in family 2 (B). Dashed line indicates the relationship by history; exact relationship is not clear (B). Unfilled shapes denote healthy while shaded shapes denote affected individuals; squares are males; circles are females; small triangle represent stillborn and double horizontal lines denote consanguineous marriages.

variants in human *IQSEC2* (MIM: 300522) are the cause of nonsyndromic and syndromic forms of X chromosome-linked intellectual disabilities (XLIDs),[21–24] whereas pathogenic variants in the autosomal *IQSEC1* have not been described yet.

Given that there is a single fly gene, *schizo*, and three human IQSEC homologs with high DIOPT scores,[8] the phenotypes of loss of *schizo* in flies are anticipated to be more severe than in human. Indeed, paralogs often functionally compensate for each other, providing genetic robustness and revealing tissue-specific phenotypes.[25]

The main known phenotype associated with loss of *schizo* is a growth cone guidance defect. Growth cones of neurons often follow precise paths to find and connect with their targets by sampling cues produced by numerous cell types.[26] The Slit-Robo (Roundabout) pathway is one of main axon guidance pathways discovered in *Drosophila*.[27–30] Slit is secreted by the midline CNS glial cells in embryos where it binds to Robo receptors expressed on growth cones of neurons to prevent them from crossing the midline in tracks named commissures.[31] The levels of Robo are then downregulated by expression of *commissureless,* an E3 ligase, expressed in neurons, permitting them to cross the midline as they do not interact with the Slit repellant and are attracted by Netrins.[32] In the midline glia, *schizo* was shown to downregulate Slit secretion.[9] Hence, in the absence of *schizo*, the increase in Slit prevents many growth cones from crossing the midline. Slits secreted by glia in mice similarly regulate the crossing of axons in the brain to form the corpus callosum, a process mediated via Robo proteins in neurons.[33] Some affected individuals with *IQSEC2* variants exhibit a thinning of the corpus callosum,[23] suggesting that the function of *schizo* may be conserved. In summary, the above data suggest that *IQSECs* and *schizo* may play similar roles in flies and vertebrates.

In this study, we report five affected individuals from two unrelated families with similar phenotypes of intellectual disability, developmental delay, short stature, aphasia, and hypotonia. By combining exome sequencing and genotyping of family members, we identified two different recessive likely pathogenic variants in *IQSEC1*, segregating in each family with the disease phenotype. Studies of the *Drosophila* ortholog and expression of cDNAs encoding human reference and variant *IQSEC1* in flies suggest that the variants are loss- or partial loss-of-function mutations. Finally, loss of IQSEC1 in neurons of the mouse cortex leads to defects in the maturation of dendritic spines. The model organism data underscore the importance of Schizo in flies and IQSEC1 in mice, orthologs of human IQSEC1, in neural development and function.

Material and Methods

Families Studied

Family 1 (F208) was enrolled, recruited, and sampled by the Institute of Basic Medical Sciences (IBMS), Khyber Medical University, Peshawar, Pakistan, and was studied at the Department of Genetic Medicine and Development, University of Geneva, Switzerland. The current study was approved by the ethical committee of the Khyber Medical University, Peshawar, Pakistan and by the Bioethics Committee of the University Hospitals of Geneva (Protocol number: CER 11-036). Family 2 was studied at the National Neuroscience Institute, King Fahad Medical City, Riyadh, Saudi Arabia, after the ethical approval of the institution. Informed consent forms were signed by guardians of both families. Peripheral blood samples were obtained from individuals of both families and the genomic DNA was extracted according to standard protocols.

Genetic Analysis

In family 1 (F208), whole-exome sequencing of the proband (IV-2, Figure 1A) was performed by using SureSelect Human All Exon v6 reagents (Agilent Technologies) and sequenced on an Illumina HiSeq4000 platform. The exome-sequencing data were analyzed by using a customized pipeline that includes the published algorithms, Burrows-Wheeler aligner tool (BWA),[34] SAMtools,[34] PICARD, and the Genome Analysis Toolkit (GATK).[35] Sequenced reads were aligned to the GRCh37/hg19[36] reference human genome and the filtering of variants was performed as described in previous studies.[37–39] The Illumina 720K SNP array (HumanOmniExpress Bead Chip by Illumina) was performed to genotype the members of the family (III-1, III-2, IV-2, IV-3, and IV-6 in Figure 1A) that were sampled. The genotyping data were analyzed to calculate the run of homozygosity (ROH) by using PLINK.[40] A homozygous region of 50 consecutive

homozygous SNPs, allowing a maximum of one mismatch and demarcated by the first heterozygous SNP at the edge, was defined as the ROH. Variants from the exome-sequencing data, present in the ROH segregating with the disease phenotype in the family, were isolated and filtered by using CATCH.[41] Features like zygosity, quality score, minor allele frequency, conservation scores, and pathogenicity prediction were used to filter and prioritize the likely pathogenic variants as described previously.[37,38,42] In two affected individuals (V-6 and V-8) in family 2, enrichment, sequencing, mapping, and variant calling were done by Beijing Genome Institute Europe (Copenhagen, Denmark). Capture of exons was done using an Agilent SureSelect Human All Exon 50 Mb Kit (V4). Sequencing was performed using an Illumina Hiseq 2000. Read mapping and variant calling were done using BWA and GATK, respectively. Annotation and variant prioritization were done as described.[43] In particular, due to parental consanguinity, homozygous variants were selected and filtered for low frequencies (less than 1%) in multiple control populations (in-house database with > 5,000 European exomes and 450 exomes from individuals from the Middle East, and the ExAC and gnomAD database) and pathogenicity of the variant (LoF variants or evolutionary conserved missense variants). This led to the identification of homozygous variants in *IQSEC1*, *DNAJC25-GNG10* (a readthrough transcript with uncertain biological relevance), and *WNT5A* (MIM: 164975) (involved in autosomal-dominant Robinow syndrome [MIM: 180700]) in family 2. Heterozygosity of the *IQSEC1* variant (the only likely candidate variant) in the parents and homozygosity in the affected sibling was done by Sanger sequencing. All candidate variants were validated by Sanger sequencing (Figure S1).

Drosophila Genetics

The following stocks were obtained from the Bloomington *Drosophila* Stock Center (BDSC) at Indiana University: y^1 *w*; Mi {MIC}siz*^{MI02011} (RRID: BDSC_38550[44]), y^1 *w*; Mi{MIC}siz*^{MI13078}*/ TM3,* Sb^1 Ser^1 (RRID: BDSC_58652[44]), y^1 *w*; Mi{MIC}siz*^{MI01727}*/ TM3,* Sb^1 Ser^1 (RRID: BDSC_35071[44]), y^1 *w*; Mi {PT-GFSTF.2} is siz*$^{MI01727\text{-}GFSTF.2}$ (RRID: BDSC_60287[45]), y^1 *w*; P {Act5C-GAL4} 25FO1/CyO, y+* (RRID: BDSC_4414[46]), *P {w [+mW.hs] = GawB} elav[C155]* (RRID: BDSC_458[47]), y^1 v^1*; P{TRiP.HMS01980} attP40/ CyO* (RRID: BDSC_39060[48]), and P{KK103616} VIE-260B (RRID: VDRC[49]).

To test whether the RNAis are specific for *schizo*, we tested two independent RNAi stocks (TRiP.HMS01980 and KK103616) that should target all transcripts. Both cause embryonic lethality when ubiquitously expressed with *Act-Gal4* or *Repo-Gal4* but are viable when crossed to *elav-Gal4*, suggesting that they target *schizo*.

Generation of IQSEC1 *Drosophila* Transgenes

Transgenic stocks were generated as previously described.[50] Briefly, the *IQSEC1* cDNA entry clone (GenBank: NM_001330619.1) was shuttled to the pGW-attB-HA[51] using Gateway cloning (Thermo Fisher Scientific). Q5 site-directed mutagenesis (NEB) followed by Sanger verification was used to create IQSEC1 variants with the following primers: IQSEC1-T235M, FW 5′-GACACGGACAT GAGCTGCCGG-3′, RV 5′-AGCCTTGTCCTCTTTGTGGG-3′; IQSEC1-R213Q, FW 5′-CTGCGGCTACAGGCTGGGGGC-3′. RV 5′-GTCCGACTCGGTGCTGGAC-3′ Constructs were inserted into the VK37 (PBac {y [+] – attP } VK00037) docking site by Phi-C31-mediated transgenesis.[52]

Hatching Rate Experiments and Immunohistochemistry of Embryos

To quantify the hatching rate of embryos, we collected freshly laid eggs for 4 h on grape juice plates.[53] The hatched larvae were counted after 2 days. Larval stages were assessed based on the size of the mouth hooks.

For immunohistochemistry, embryos were collected and processed using the formaldehyde-based fixation protocol.[53] Embryos were incubated in CY3 conjugated goat anti-HRP antibody (Jackson ImmunoResearch #123-165-021) diluted 1:250 in PBS-Tween (0.1 %) with 10% NGS solution on a rotating platform overnight at 4°C in the dark. Embryos were washed in PBS-Tween (0.1%) and mounted in ProLong Gold Antifade Mountant (ThermoFisher). Confocal images were taken using a SP8 confocal microscope (Leica) with a 20× or 63× oil immersion lens. Image analysis and processing was performed using Imaris 9.3.0 (Bitplane).

ERG Recording of Fly Eye

ERG (electroretinogram) recordings were performed as described in Verstreken et al.[54] In brief, flies were glued to a slide with Elmer's Glue. A recording electrode filled with 100 mM NaCl was placed on the eye, and a reference electrode was placed on the fly head. During the recording, a 1 s pulse of light stimulation was given, and the ERG traces of ten flies for each genotype were recorded and analyzed with WinWCP v.5.3.3 software.

Dendritic Spines in Brain Sections of Mice with a Conditional *Iqsec1* Deletion in Cortical Neurons

All animal procedures were in accordance with the European Union's Directive 86/609/EEC and the Regional Boards in Hamburg and Berlin (T-0269/11). To deplete IQSEC1 in cortical projection neurons and to label a subset of neurons, we crossed *Iqsec1*$^{fl/fl}$ mice[15] with *NEX-Cre* mice[55] and *thy1-GFP* line M mice.[56] IQSEC1 was detected in cortex protein samples (7 μg total protein/lane) from wild-type, *Iqsec1*$^{fl/fl}$*:NEX-Cre*-negative (ctrl) and *Iqsec1*$^{fl/fl}$*:NEX-Cre*-positive (ΔIQSEC1) mice on an immunoblot as described.[15]

Sagittal slices (100 μm) of 4 pairs of male littermate mice (2–4 months) were prepared using a vibratome (VT 1000S, Leica), imaged, and analyzed blind to genotype. GFP-positive layer V pyramidal neurons of the somatosensory cortex were identified on an SP5 inverted confocal laser-scanning microscope system (Leica). Z stack images (step size: 0.5 μm) of 488 nm-argon-laser-scanned image fields (pixel size x,y: 0.05 μm) with segments of secondary dendrites branching into cortical layer II/III were acquired using a 63-times magnifying oil-immersion objective with a 1.25 numerical aperture and a 5-times optical zoom. Blind 3D deconvolution was performed on all z stacks using Autoquant X3 (Media Cybernetics). Spines were detected and their body lengths (largest distance to the surface of the dendrite model) and head diameters evaluated by NeuronStudio (CNIC, Mount Sinai School of Medicine) until an equal number of spines (1,917) per genotype was reached. Only automatically recognized spines were analyzed.

Spine densities, body lengths, and head diameters determined in 47 (ctrl) and 39 (ΔIQSEC1) dendritic segments of 4 mice per genotype were plotted as boxplots with Min-to-Max-whiskers. Graph Pad Prism version 5 was used for graphs and statistical analysis. Statistical significances (*$p < 0.05$) for differences between genotypes were assessed via t test.

Table 1. Clinical Features of Affected Individuals with Recessive *IQSEC1* Variants

Family ID	**Family 1 (F208)**		**Family 2**		
Variation in IQSEC1 (NM_001134382.3)	**c.1028C>T (p.Thr343Met) Homozygous**		**c.962G>A (p.Arg321Gln) Homozygous**		
Origin	**Pakistani**		**Saudi Arabia**		
Individual ID	IV-2	IV-6	V-1 (not genotyped)	V-6	V-8
Sex	female	female	male	male	male
Age at last evaluation (years)	36	23	6	11	6
Height (cm)	146	150	120	148	119
Stature	short	short	short	short	short
Head circumference (cm)	51 (<1 percentile)	51 (<1 percentile)	48 (25th percentile)	53 (50th percentile)	49 (25th percentile)
Intellectual disability	severe	severe	severe	severe	severe
Developmental delay	yes	yes	yes	yes	yes
Speech	aphasia	aphasia	few words	few words	few words
Motor milestones	delayed	delayed	delayed	delayed	delayed
Epilepsy	no	no	yes (early on-set)	yes (early on-set)	yes (early on-set)
Hypotonia	yes (mild)	yes (mild)	yes	yes	yes
Behavioral problems	aggressive	aggressive	inattention and hyperactivity	aggressive, ADHD and hyperactivity	inattention and hyperactivity
MRI	not done	not done	normal	normal (figure s2)	normal
Other symptoms	low vision	lower limbs weakness	multiple hyperpigmented café au lait spots in his lower back and upper thigh, truncal ataxia and ataxic gait with frequent falls	unsteady gait	unsteady gait

Abbreviations: ADHD, attention deficit hyperactivity disorder; MRI, magnetic resonance imaging.

Results

Clinical Evaluation of Affected Individuals

As shown in Figure 1A, family 1 (F208) is a consanguineous family. It originates from the region near Kohat in Khyber Pakhtunkhwa, Pakistan. In this family there were four affected individuals and two of them died at an early age with unknown etiology except that they shared many features, including ID, short stature, microcephaly, aphasia, and aggressive behavior, with the two surviving individuals. As indicated in the pedigree, the unaffected parents (III-1 and III- 2) are first cousins (Figure 1A). Of their seven children, four are affected (IV-2, IV-4, IV-6, and IV-8) and three are healthy (IV-1, IV-3, and IV-7); one pregnancy was interrupted naturally for unknown reason (IV-5). Among the affected siblings, two (IV-2 and IV-6) were alive at the time of evaluation. Both individuals exhibit similar phenotypes of severe intellectual disability, short stature, aphasia, hypotonia, facial dysmorphisms, and aggressive behavior (Table 1). Three affected siblings (two brothers and one sister) of the father (III-1) had died for an unknown genetic disorder.

In family 2 from Saudi Arabia, three male affecteds (V-1, V-6, and V-8), aged 6, 11, and 6 years, respectively, presented with a history of severe epileptic encephalopathy, delayed psychomotor development and ID (Figure 1B). The phenotypically unaffected parents (III-4 and IV-3) are consanguineous (first cousins once removed). The affected individual (V-7) died at age 6 without genetic diagnosis, but his presentation of disease and symptomatic course were similar to his affected brothers. There is a paternal family history of seizure disorder and brain atrophy. The unaffected siblings (V-2, V-3, V-4, and V-5) showed neither evidence of epilepsy nor major cognitive or motor deficits. The seizures in affected individuals (V-1, V-6, V-7, and V-8) started at 2 months of age with brief jerky-like movements. They developed febrile seizures, which were soon followed by other seizure types including predominant generalized tonic-clonic seizures and absence seizures. They also exhibited repeated episodes of status epilepticus triggered by illnesses or fever. Despite multiple medication trials, the affected individuals continued to experience multiple seizures of different semiology many times per day. They were able to walk independently at age 3 and started to use short phrases before the age of 4. With time they showed behavioral changes in the form of hyperactivity and/or lack of attention. Brain MRI scans and EEG (electroencephalography) performed in the two affected individuals of family 2 did not reveal any abnormality (no thinning of the corpus

callosum) (Figure S2). Follow-up EEG studies showed a slowing of the background activity, diffuse delta, and some theta activity. Low-amplitude sharp discharges were seen at the front central regions of brain.

In summary, affected individuals from both families shared similar clinical features, including intellectual disability, developmental delay, short stature, hypotonia, and aphasia.

Exome Sequencing and Genetic Analyses Reveal Missense Variants in *IQSEC1*

Exome sequencing was first performed in proband IV-2 of family 1 (F208) with a coverage of >95% at 20× and a total mean coverage of ~100×. The data were analyzed by using our in-house pipeline and prioritization algorithm.[37,38] This yielded no pathogenic variants in genes known to be implicated in intellectual disability, developmental delay, or short stature. We then intersected the exome-sequencing data with the genotyping data of five members of family 1 (F208) to select variants in the regions of homozygosity (ROH) segregating recessively with the disease phenotype. All segregating variants were filtered as described previously.[37,38] We included homozygous exonic and splicing variants (±6 bp), excluded all synonymous variants, except in the splicing regions, selected variants with a minor allele frequency of <0.02 in gnomAD database[57] and our local control subjects, filtered out if found within duplications of the genome, conservation score (by GERP++),[58] and predicted pathogenicity scores (by SIFT,[59] PolyPhen2,[60] and Mutation Taster[61]) were also taken into account. Using the above mentioned filters, only one homozygous missense variant (GenBank: NM_001134382.3; c.1028C>T [p.Thr343Met]) in *IQSEC1* was identified in IV-2 and IV-6 of family 1 (F208) (Figures 1A and S1A). The number of heterozygous IQSEC1 loss-of-function variants in gnomAD is low. Hence, the pLI score of IQSEC1 calculated in gnomAD is 1, indicating that the gene is intolerant to loss-of-function variants. The absence of homozygous loss-of-function variants in gnomAD also suggests that the presence of bi-allelic loss-of-function variants is incompatible with normal life. As such, the homozygous missense variants described here may represent partial loss-of-function variants causing recessive disease. The *IQSEC1* variant p.Thr343Met is present twice in 230,690 alleles in gnomAD and missing in the Bravo database (125,568 alleles). However, no homozygous variant was found in these databases. Moreover, the variant was not present in our local cohort of 300 control subjects from the same Pakistani ethnicity. Segregation of the variant was confirmed by Sanger sequencing; the variant is heterozygous in parents (III-1 and III-2) and homozygous in both affected individuals (IV-2 and IV-6) and the unaffected sibling (IV-3) is normal and not carrying the variant (Figures 1 and S1). By sharing our findings through GeneMatcher,[62] we found the second family (family 2) with three affected individuals from Saudi Arabia with a different homozygous missense variant (c.962G>A [p.Arg321Gln]) and similar clinical findings. Again, both parents (III-4 and IV-3) were carriers and the affected children (V-6 and V-8) were homozygous (Figure S1B). This variant is present 2-fold in Bravo and three times in gnomAD databases. The phenotype of the affected individual (V-1) from different parents is very similar to individuals V-6 and V-8, but a DNA sample was unavailable to document the segregation of IQSEC1 variant p.Arg321Gln.

The Human Variants of *IQSEC1* Behave as Loss-of-Function Mutations in *Drosophila*

The fly homolog of *IQSEC1*, *IQSEC2*, and *IQSEC3* (MIM: 612118) is *schizo*; however, Schizo shows a slightly higher sequence similarity to IQSEC1 than to IQSEC2 and IQSEC3 (DIOPT score of 12, 11, and 9 out of 15,[8,63,64] respectively). Schizo and IQSEC1 share 45% similarity and 32% identity over their entire proteins and contain a well-conserved Sec7 and PH domain (Figure 2A). To examine whether the *IQSEC1* variants impair the function of the protein, we generated UAS-transgenes with the *IQSEC1* variants (p.Thr343Met, p.Arg321Gln) as well as the reference *IQSEC1* cDNA. Ubiquitous overexpression of the reference *IQSEC1* cDNA in wild-type flies is lethal, showing that overexpression is toxic. However, wild-type animals overexpressing either of the two *IQSEC1* variant cDNAs were viable, showing that the variants are likely to be loss-of-function variants (Figure 2B).

To study the function of *schizo*, we used four different Minos Mediated Integration Cassette (MiMIC) insertions.[44,65] As shown in Figure 2C, MiMICs contain the *yellow+* dominant body-color marker to identify the transgenic animals, a mutagenic gene-trap cassette consisting of a SA followed by stop codons, the coding sequence of the fluorescent protein EGFP, and an SV40 polyadenylation signal sequence. The sequences between the *attP* sites can be replaced through Recombination Mediated Cassette Exchange (RMCE) *in vivo* with any DNA cassette flanked by two inverted ΦC31 attB sites. $siz^{MI13078}$ is inserted in a coding exon that targets the four transcripts of *schizo,* and $siz^{MI01727}$ is inserted in an intron truncating all *schizo* transcripts. Both insertions cause embryonic lethality, but $siz^{MI02011}$, which only targets one transcript (RB), does not cause lethality indicating that RB is not critical for survival (Figure 2C). As expected, $siz^{MI13078}$ fails to complement $siz^{MI01727}$. To assess the endogenous subcellular localization of the Schizo protein, we integrated the artificial exon SA-EGFP-FlAsH-StrepII-TEV-3xFlag tag-SD flanked by two inverted attB sites ($siz^{MI01727\text{-}GFSTF.2}$; *siz-GFP*) (Figure 2C). These flies are homozygous, viable, and healthy, indicating that the internal GFP tag does not obviously affect protein function and that the $siz^{MI01727}$ chromosome carries no other lethal or visible mutations.

Given that overexpression of the reference *IQSEC1* cDNA is toxic, we lowered the overexpression of human reference and variant cDNAs by raising the mutant animals at 18°C and found that the reference human cDNA

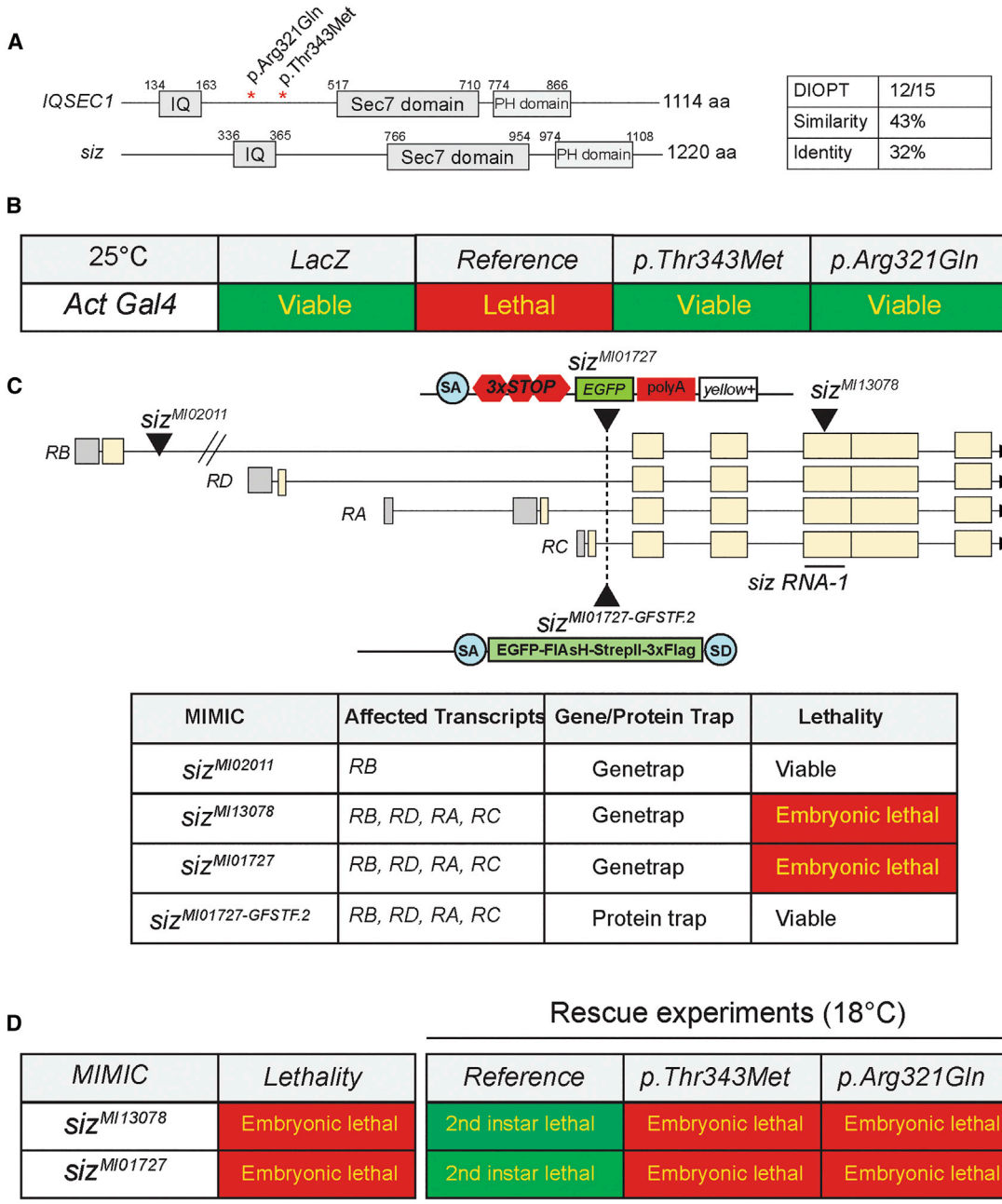

MIMIC	Affected Transcripts	Gene/Protein Trap	Lethality
$siz^{MI02011}$	RB	Genetrap	Viable
$siz^{MI13078}$	RB, RD, RA, RC	Genetrap	Embryonic lethal
$siz^{MI01727}$	RB, RD, RA, RC	Genetrap	Embryonic lethal
$siz^{MI01727\text{-}GFSTF.2}$	RB, RD, RA, RC	Protein trap	Viable

MIMIC	Lethality	Reference	p.Thr343Met	p.Arg321Gln
$siz^{MI13078}$	Embryonic lethal	2nd instar lethal	Embryonic lethal	Embryonic lethal
$siz^{MI01727}$	Embryonic lethal	2nd instar lethal	Embryonic lethal	Embryonic lethal

Figure 2. Schizo Is a Functional Homolog of IQSEC1 in Fly
(A) Schizo and IQSEC1 are evolutionarily conserved and share IQ-like motif, Sec7, and PH domains.
(B) Overexpression of *IQSEC1* at 25°C is toxic, but the human IQSEC1 variants are not toxic when expressed under the same conditions.
(C) Structure of *schizo* and its transcripts. MiMIC transposable element insertions in *schizo* are embryonic lethal. The MiMIC $siz^{MI01727}$ was converted using RMCE and an artificial exon that encodes GFP was introduced ($siz^{MI01727\text{-}GFSTF.2}$) to determine protein localization.
(D) Embryonic lethality of siz^{M13078} and $siz^{MI01727}$ are partially rescued by human *IQSEC1 WT* but not by *IQSEC1 p.Thr343Met* or *IQSEC1 p.Arg321Gln*. 0% of eggs of homozygous mutants ($siz^{MI13078}$ and $siz^{MI01727}$, n > 500) hatched. At room temperature, 70% (n = 120) of the eggs hatched when the *UAS-IQSEC1* reference was ubiquitously overexpressed ($siz^{MI01727}/siz^{MI01727}$*;act-Gal4/UAS-IQSEC1 ref*) but 80% (n = 84) of hatched larvae died as 2nd instar larvae (~20% of hatched larvae die in 1st instar larvae stage). None of embryos (n = 150) hatched when the *UAS-IQSEC1* variants were ubiquitously overexpressed ($siz^{MI01727}/siz^{MI01727}$*;act Gal4/UAS-IQSEC1* [p.Thr343Met or p.Arg321Gln]).

can partially rescue the lethality from embryos of $siz^{MI01727}$ and $siz^{MI13078}$ to 2nd instar larvae. However, both IQSEC1 p.Arg321Gln and IQSEC1 p.Thr343Met failed to rescue embryonic lethality, again suggesting that these variants are loss-of-function mutations (Figure 2D).

To determine where the Schizo protein levels in embryos, we costained them with anti-Repo (a glial marker) and anti-Elav (a neuronal marker) in GFP $siz^{MI01727\text{-}GFSTF.2}$ *(siz-GFP)*-expressing embryos. As shown in Figure 3A, Schizo is broadly localized in the nervous system of

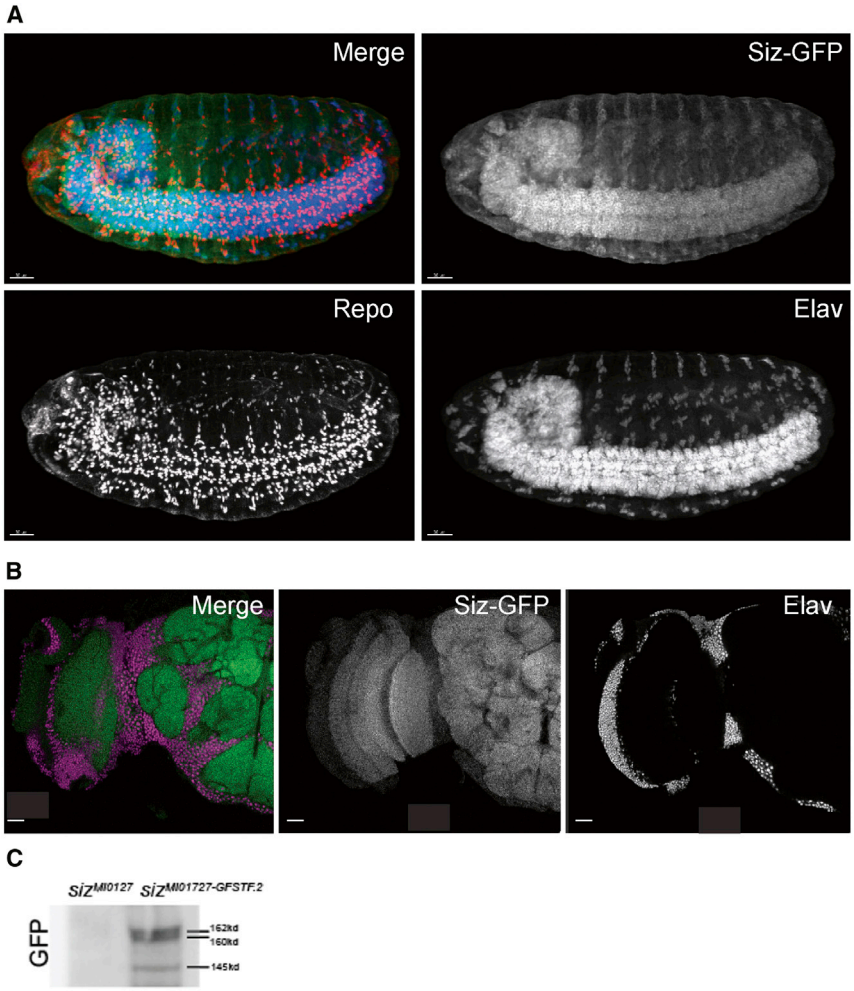

Figure 3. *Schizo* Is Localized in Glia and Neurons in Fly

(A) $siz^{MI01727\text{-}GFSTF.2}$ (*siz-GFP*) embryos were stained with anti-Repo (glia) and anti-Elav (neurons) antibodies. Siz-GFP is broadly localized in the nervous system in fly embryos, including neurons and glia. The scale bar is 50 μm.

(B) In adult heads, Siz-GFP (green) is localized in the neuropil and cell bodies of neurons and glia. Elav staining labels the nuclei of the neurons (magenta). The scale bar represents 50 μm.

(C) Analysis of lysates from *siz-GFP* flies revealed three different kinds of transcripts.

stage 15 embryos, including CNS and PNS neurons and glial cells. In the adult brain (Figure 3B, half of a *Drosophila* brain), the protein is present throughout the neuropil and cell bodies and is also localized in glia (not shown). Analysis of lysates from *siz-GFP* flies probed with a polyclonal antibody against GFP revealed three different proteins (145 kDa, 160 kDa, and 162 kDa) in agreement with the molecular mass calculated for RB, RD, and RA when fused with GFP. These proteins are not detected in $siz^{MI0127}/TM3$ animals (Figure 3C). In summary, *schizo* is localized in glia and neurons at all stages tested, including third instar larvae (not shown).

Schizo regulates Slit expression by promoting its endocytosis in CNS midline glia of embryos and hence affects commissure formation.[9] To assess the phenotype of the siz^{M01727} mutants, we collected embryos and stained them with an antibody to HRP, a marker for neuronal membranes. We observe numerous commissural defects, consistent with previous findings[9] (Figure 4A), suggesting that siz^{M01727} is a strong loss-of-function allele. However, we also noted very severe axonal guidance and dendritic projection defects in the PNS of embryos that were not previously reported (Figure 4B).

IQSEC1, IQSEC2, and IQSEC3 are localized in the mouse retina.[66,67] Given that Schizo is also localized in photoreceptors (Figure 3B), we performed electroretinography (ERG) to determine whether the protein is required in the fly visual system. While ubiquitous or glia-specific downregulation of *schizo* is lethal, neuron-specific downregulation of *schizo* produces viable flies. We lowered expression of *schizo* using two independent RNAis (*elav > siz RNAi-1* (TRIP.HMS01980) and *elav > siz RNAi-2* (P{KK103616})) and performed ERG recordings in 5-day-old flies. As shown in Figure 5, reduced expression of *schizo* dramatically affect ERG amplitude and abolished the on- and off-transients when compared to controls (*elav > Luciferase RNAi*). Hence, vision of these flies is either very severely impaired or lost.

Targeted Depletion of IQSEC1/BRAG2 in Mouse Cortex Neurons Affects the Maturation of Dendritic Spines

In the mammalian CNS, IQSEC1 is concentrated in postsynaptic densities and plays a critical role in the development and plasticity of glutamatergic synapses.[15,16,20] Dysgenesis of dendritic spines,[68–70] which house the postsynaptic specializations of glutamatergic synapses, represents a morphological hallmark of disorders associated with intellectual disability and autism.[71,72] To explore a role of IQSEC1 in the development of dendritic spines in the neocortex, we generated *Iqsec1*-floxed mice[15] carrying both a *NEX-Cre* allele that drives Cre expression in projection neurons of the cortex[55] and a *thy1-GFP* allele (*thy1-GFP* line M) that labels a subset of cortical cells.[73] In cortices of *NEX-Cre*-positive *Iqsec1*-floxed mice, we detected only traces of IQSEC1/BRAG2 protein (Figure 6A), confirming that *NEX-Cre*-mediated deletion of exon 2 in *Iqsec1* early in development suppressed IQSEC1 expression in cortical neurons to a large extent. We chose to analyze spines on secondary apical dendrites of GFP-positive

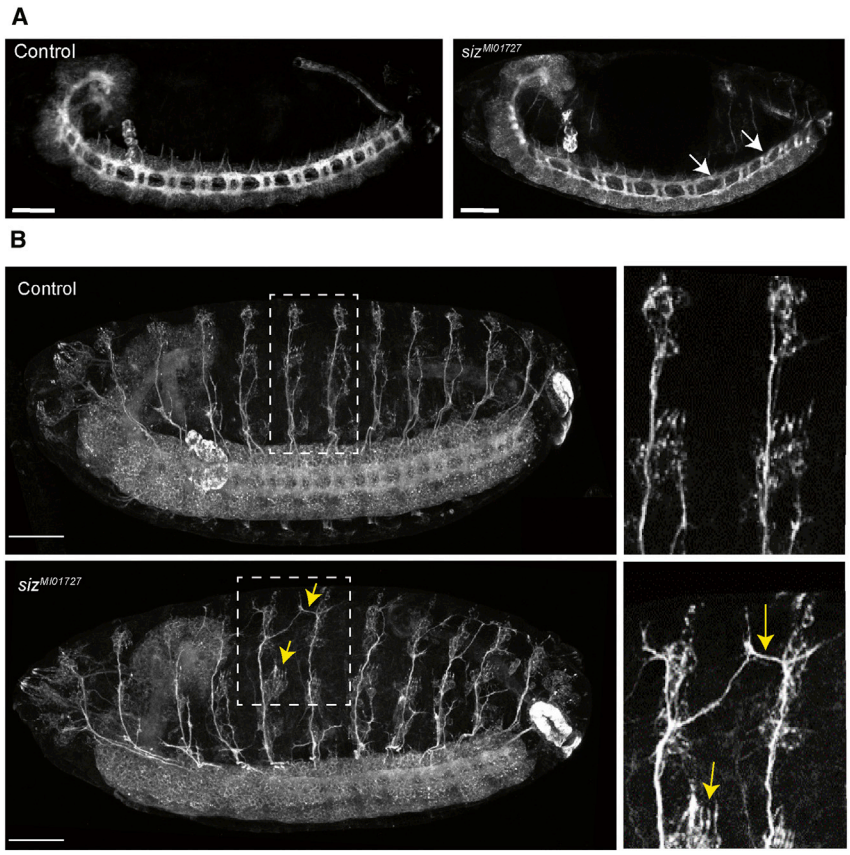

Figure 4. *Schizo* Is Required for Proper Axon Guidance in CNS and PNS
(A) Homozygous $siz^{MI01727}$ embryos show commissural defects (white arrows).
(B) Homozygous $siz^{MI01727}$ embryos exhibit severe axonal guidance defects in the peripheral neurons of all segments (yellow arrows). The scale bar represents 50 μm.

somatosensory cortex layer V neurons in brain sections of adult Cre-positive mice (ΔIQSEC1) and Cre-negative littermates (ctrl) (Figures 6B–6H). Neurons lacking IQSEC1 had an increased density of dendritic spines (Figure 6C). Morphological measurements of 1,917 spines from each ΔIQSEC1 and ctrl mice revealed that the average body length of the spines was not altered by IQSEC1 depletion (Figure 6D). In contrast, the spines of IQSEC1-lacking neurons had on average smaller heads than the spines of ctrl neurons (Figure 6E). Depletion of IQSEC1 increased the density of spines over the whole range of the spine body lengths (Figure 6F), but the increased density was limited to spines with small heads (Figure 6G). Together, IQSEC1-deficient layer V neurons contained excess spines with small heads in adult mice. We divided the spine head diameter by the spine body length to reveal a maturity index for each spine and evaluated the effect of the genotype (Figure 6H). The leftward shift of the cumulative frequency curve upon IQSEC1 depletion indicates that lack of IQSEC1 in cortical neurons leads to an increase in immature-appearing dendritic spines.

Discussion

We report five affected individuals from two unrelated families having different pathogenic bi-allelic recessive variants in *IQSEC1*; all case subjects present similar clinical features: intellectual disability, short stature, and speech problems. Additionally, the three affected individuals from family 2 harboring IQSEC1 p.Arg321Gln present with seizures. The inclusion of the *IQSEC1* locus in clinical diagnosis may identify more affected individuals with pathogenic variants in *IQSEC1* that would enable the description of this gene-phenotype link and potentially reveal genotype-phenotype correlations.

Mutations in *IQSEC2* have been linked to XLIDs. Initially, inherited mutations in *IQSEC2* were identified in four families with non-syndromic ID.[24] These missense mutations resulted in amino acid changes in the Sec7 domain or IQ-like motif and in a compromised GEF activity of IQSEC2 on ARF6.[21,74] Subsequently, *IQSEC2* mutations have also been found in affected individuals with syndromic forms of ID with seizures, and many of the pathogenic variants in *IQSEC2* were shown to occur *de novo*.[22,23,75–79] Taken together, familial and *de novo* mutations in *IQSEC2* are associated with moderate to profound ID and with seizures. Mutations in *IQSEC3* have recently been found in families with ID as well.[80]

The three IQSECs in human (1, 2, and 3) are highly similar in structure and sequence. They also show similar sequence identities to the fly Schizo protein even though IQSEC1 has the highest DIOPT score when aligned with Schizo.[8,63] Loss of *schizo* in flies causes embryonic lethality whereas homozygous loss-of-function variants in *IQSEC1* (this work), *IQSEC2*,[22,23] and *IQSEC3*[80] are recessive and do not appear to cause lethality. This is anticipated as essential genes in flies with neural phenotypes with more than one human homolog were three times more likely to be associated with human diseases reported in OMIM.[81–83] In contrast, most of the essential fly genes with a single human homolog were not reported in OMIM[82] as they may be essential in human as well. Hence, one simple interpretation would be that the three IQSECs are partially redundant in vital functions. It is also worth noting that the phenotypes associated with the mutations in the three human *IQSEC* genes are quite similar: intellectual disability, short stature, and speech problems.[22,23,80]

The claim that the pathogenic variants in *IQSEC1* are causative is supported by the overexpression assays, rescue experiments, protein localization, and phenotypic data

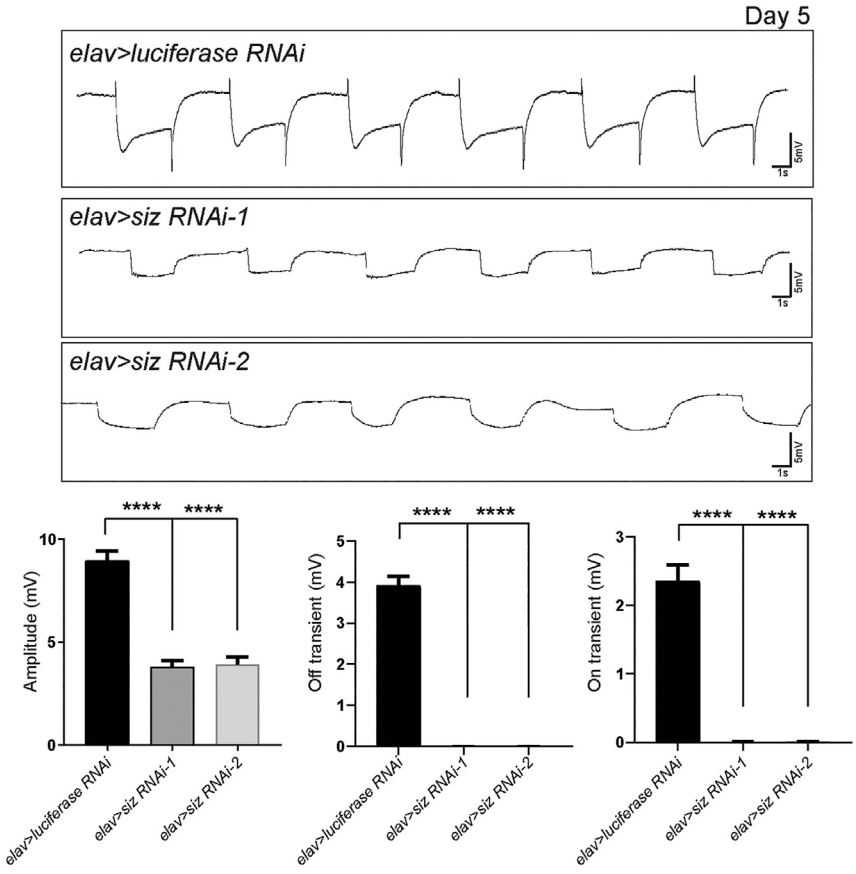

Figure 5. *Schizo* Is Required in the Fly Visual System
Lowering the level of Schizo in neurons (*elav > siz RNAi-1 and elav > siz RNAi-2*) caused dramatically reduced amplitudes and loss of on- and off-transients of ERGs when compared to control (*elav > Luciferase RNAi*). Statistical analyses are one-way ANOVA followed by a Tukey post hoc test. Mean ± SEM; ****$p < 0.001$.

associated with the loss of the homolog of *IQSEC1*, *schizo*, in fly embryos. The human *IQSEC1* variants result in amino acid changes in the region between the IQ-like motif and the Sec7 domain. While Schizo and IQSEC1 show high sequence similarities between the functional domains, this region is not well conserved between *Drosophila* and human. Nevertheless, both variants present a clear functional difference when overexpressed compared to overexpression of reference cDNA. The mutations are unlikely to affect the basal GEF activity of IQSEC1, since they are located outside of the Sec7 domain. However, the regulation of the GEF activity by Ca^{2+}/Calmodulin and by surface receptors[18,20] may be impaired in the IQSEC1 variants. Alternatively, they may affect protein folding, alter subcellular localization, or reduce protein stability.

Loss of *schizo* causes severe axonal guidance defects in the CNS[9] but we also observe severe axon and dendritic defects in the PNS. In the PNS the axons are often short and highly aberrant in structure and aberrant axon outgrowth was also described for *in vitro* cultured cortical neurons derived from *Iqsec2* knockout mice.[84] Note that the Slit and Robo proteins as well as Arf6 are known to play a critical role in the formation of the corpus callosum in mice[85] and these proteins control crossing of growth cones across the midline in mice,[33] similar to the formation of commissures in flies. Finally, a conserved function in myoblast fusion has been described for Schizo and IQSEC1.[11,86]

Given that the mouse homologs of IQSECs are localized in the eye[66,67] and *schizo* is localized in the fly photoreceptors, we also recorded ERGs upon knockdown of *schizo* in photoreceptor neurons. These flies exhibit almost complete loss of ERG amplitudes and lack of on-off transients, showing that they have no or severely impaired sight. Interestingly, vision defects have also been documented in affected individual IV-2 of family 1 (this study) and in *IQSEC2* case subjects.[22,23]

IQSEC1 and IQSEC2 are core components of the postsynaptic density at excitatory synapses in the brain.[13–16] Genes for postsynaptic density proteins are frequently linked to cognitive disorders.[87] Both IQSEC1 and IQSEC2 are controlled by NMDA receptors and are critical for the activity-dependent reduction in the efficacy of AMPA receptor-mediated synaptic transmission during long-term depression.[15,17,18,20,88,89] IQSECs function as GEFs for the small GTPase Arf6 that controls endosomal protein traffic and actin cytoskeleton reorganization at the plasma membrane. Arf6 regulates the development of dendritic spines by promoting the conversion of filopodia into spines.[90,91] We previously observed that a targeted reduction of IQSEC1 or IQSEC2 levels interferes with the maturation of glutamatergic synapses.[20] Here, we show that a depletion of IQSEC1 in neurons of the mouse cortex affects the density and morphology of dendritic spines. In hippocampal neuron cultures, a knockdown of *Iqsec2* expression resulted in a transiently increased density of dendritic spines at DIV15, whereas overexpression of *IQSEC2* resulted in an increased proportion of mature spines at DIV21.[84] The increased density and immature-appearing morphology of the dendritic spines of IQSEC1-depleted neurons of the cortex support a direct role of IQSEC1 in the development of dendritic spines. Spine dysgenesis has been connected with ID previously.[71] The link between lack of IQSEC1 and aberrant spine development therefore supports that loss-of-function variants of IQSEC1 can cause ID.

In summary, we describe a syndrome associating intellectual disability, developmental delay, short stature,

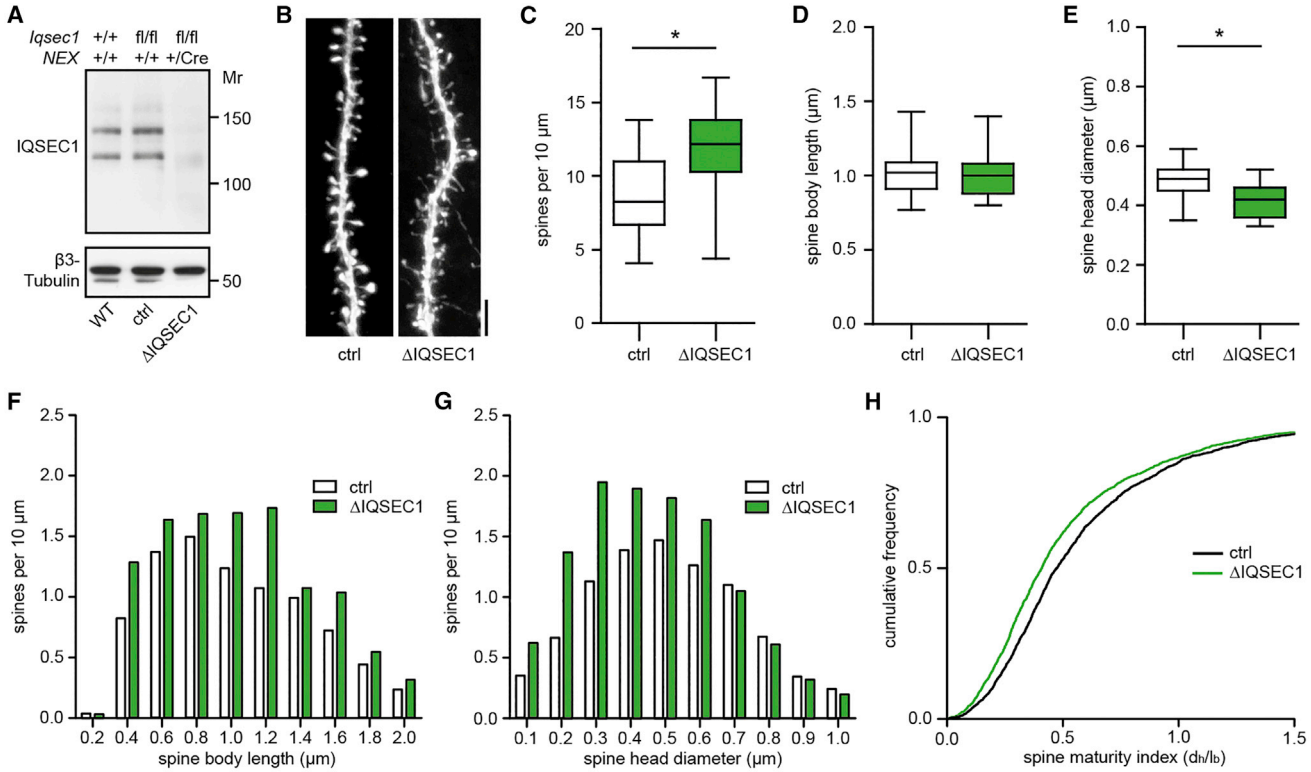

Figure 6. IQSEC1 Depletion in Mouse Cortex Results in Dendritic Spines of Immature Morphology
(A) Western blot revealing IQSEC1 in the cerebral cortex of wild-type (WT), *NEX-Cre*-negative (ctrl), and *NEX-Cre*-positive (ΔIQSEC1) *Iqsec1*$^{fl/fl}$ mice.[15]
(B) Representative images of dendritic segments of cortical layer V neurons of *thy1-GFP*-positive ctrl and ΔIQSEC1 mice. Scale bar: 5 μm.
(C) Spine density was increased upon IQSEC1 depletion. n = 39–47 dendrites of four mice per genotype, *p < 0.0001.
(D) Spine body length was not changed upon IQSEC1 depletion. n = 39–47 dendrites, p = 0.868.
(E) Spine head diameter was decreased upon IQSEC1 depletion. n = 39–47 dendrites, *p < 0.0001.
Data in (C)–(E) are represented as total range (whiskers), interquartile range (box), and median (line inside box).
(F and G) Density of spines with small heads (spine head diameter < 0.6 μm) was selectively increased upon IQSEC1 depletion. Shown are the densities of spines grouped into body length bins of 0.2 μm (F) or grouped into head diameter bins of 0.1 μm (G). Values on x-axes indicate the maximum of each bin.
(H) Cumulative frequency distribution of spine maturity index (0.0–1.5), calculated as the ratio of head diameter (d_h) to body length (l_b) of each individual spine of the analyzed population (ctrl, n = 1,812; ΔIQSEC1, n = 1,821), shifted to the left upon IQSEC1 depletion.

aphasia/speech problems, hypotonia, and epilepsy in some case subjects by reporting five individuals from two unrelated families harboring bi-allelic variants in *IQSEC1*. Based on experiments in *Drosophila* and mice, IQSEC1 plays a critical role in neuronal development, supporting that the bi-allelic pathogenic variants in the *IQSEC1* gene cause the above-mentioned syndrome in humans.

Supplemental Data

Supplemental Data can be found online at https://doi.org/10.1016/j.ajhg.2019.09.013.

Acknowledgments

We thank the Swiss Government Excellence Scholarships program, which provided M.A. the opportunity to work at University of Geneva Medical School in Switzerland. This project was partially supported by ERC grant 219968 and the ChildCare Foundation to S.E.A. We are thankful to all the members of the families reported in this study and the Vital-IT platform for the computational support. H.J.B. is an investigator of the Howard Hughes Medical Institute and H.C. is supported by HHMI. H.J.B. is supported by R24OD022005 from ORIP and R01GM067858 from NIGMS. Confocal microscopy was performed in the neurovisualization core of the Baylor College of Medicine Intellectual and Developmental Disabilities Research Center (supported by National Institute of Child Health and Human Development [NICHD] grant U54HD083092). *Drosophila* stocks were obtained from the Bloomington Stock Center (NIH P40OD018537) at Indiana University. Monoclonal antibodies were obtained from the Developmental Studies Hybridoma Bank, created by the NICHD, and maintained at the University of Iowa. This work was supported by the Deutsche Forschungsgemeinschaft (DFG, grant KO 2290/2-1 and Heisenberg fellowship KO 2290/1-1 to H.-C.K.) and by the Chica and Heinz Schaller (CHS) Foundation (short-term fellowship to H.C.K.). T.A.R. is supported by The Cullen Foundation. P.C.M. is funded by CIHR (MFE-164712). The dendritic spine data are part of the doctoral thesis of M.N.E. We thank Klaus-Armin Nave (Max Planck Institute for Experimental Medicine, Göttingen, Germany) for providing *NEX-Cre* mice, Joshua Sanes (Center for Brain Science, Harvard University) for sharing thy1-GFP mice, Jörg-Michael

Breustedt for help with NeuronStudio, and Janina Sülflow and Katrin Büttner for technical assistance.

Declaration of Interests

The authors declare no competing interests.

Received: July 1, 2019
Accepted: September 11, 2019
Published: October 10, 2019

Web Resources

Bravo database, https://bravo.sph.umich.edu/freeze5/hg38/
DIOPT, https://www.flyrnai.org/cgi-bin/DRSC_orthologs.pl
ExAC Browser, http://exac.broadinstitute.org/
FlyBase, http://flybase.org/
GenBank, https://www.ncbi.nlm.nih.gov/genbank/
GeneMatcher, https://genematcher.org/
gnomAD Browser, https://gnomad.broadinstitute.org/
GTEx Portal, https://www.gtexportal.org/home/
MARRVEL, http://marrvel.org/
OMIM, https://www.omim.org/
Picard, http://broadinstitute.github.io/picard/
RRID, https://scicrunch.org/resources

References

1. Willemsen, M.H., and Kleefstra, T. (2014). Making headway with genetic diagnostics of intellectual disabilities. Clin. Genet. *85*, 101–110.
2. Riazuddin, S., Hussain, M., Razzaq, A., Iqbal, Z., Shahzad, M., Polla, D.L., Song, Y., van Beusekom, E., Khan, A.A., Tomas-Roca, L., et al.; UK10K (2017). Exome sequencing of Pakistani consanguineous families identifies 30 novel candidate genes for recessive intellectual disability. Mol. Psychiatry *22*, 1604–1614.
3. Ropers, H.H. (2007). New perspectives for the elucidation of genetic disorders. Am. J. Hum. Genet. *81*, 199–207.
4. Antonarakis, S.E., and Beckmann, J.S. (2006). Mendelian disorders deserve more attention. Nat. Rev. Genet. *7*, 277–282.
5. Bittles, A.H., and Black, M.L. (2010). Evolution in health and medicine Sackler colloquium: Consanguinity, human evolution, and complex diseases. Proc. Natl. Acad. Sci. USA *107* (*Suppl 1*), 1779–1786.
6. Iqbal, Z., and van Bokhoven, H. (2014). Identifying genes responsible for intellectual disability in consanguineous families. Hum. Hered. *77*, 150–160.
7. Abou Jamra, R., Wohlfart, S., Zweier, M., Uebe, S., Priebe, L., Ekici, A., Giesebrecht, S., Abboud, A., Al Khateeb, M.A., Fakher, M., et al. (2011). Homozygosity mapping in 64 Syrian consanguineous families with non-specific intellectual disability reveals 11 novel loci and high heterogeneity. Eur. J. Hum. Genet. *19*, 1161–1166.
8. Wang, J., Al-Ouran, R., Hu, Y., Kim, S.Y., Wan, Y.W., Wangler, M.F., Yamamoto, S., Chao, H.T., Comjean, A., Mohr, S.E., et al.; UDN (2017). MARRVEL: Integration of Human and Model Organism Genetic Resources to Facilitate Functional Annotation of the Human Genome. Am. J. Hum. Genet. *100*, 843–853.
9. Onel, S., Bolke, L., and Klämbt, C. (2004). The Drosophila ARF6-GEF Schizo controls commissure formation by regulating Slit. Development *131*, 2587–2594.
10. Dottermusch-Heidel, C., Groth, V., Beck, L., and Önel, S.F. (2012). The Arf-GEF Schizo/Loner regulates N-cadherin to induce fusion competence of Drosophila myoblasts. Dev. Biol. *368*, 18–27.
11. Chen, E.H., Pryce, B.A., Tzeng, J.A., Gonzalez, G.A., and Olson, E.N. (2003). Control of myoblast fusion by a guanine nucleotide exchange factor, loner, and its effector ARF6. Cell *114*, 751–762.
12. D'Souza, R.S., and Casanova, J.E. (2016). The BRAG/IQSec family of Arf GEFs. Small GTPases *7*, 257–264.
13. Murphy, J.A., Jensen, O.N., and Walikonis, R.S. (2006). BRAG1, a Sec7 domain-containing protein, is a component of the postsynaptic density of excitatory synapses. Brain Res. *1120*, 35–45.
14. Sakagami, H., Sanda, M., Fukaya, M., Miyazaki, T., Sukegawa, J., Yanagisawa, T., Suzuki, T., Fukunaga, K., Watanabe, M., and Kondo, H. (2008). IQ-ArfGEF/BRAG1 is a guanine nucleotide exchange factor for Arf6 that interacts with PSD-95 at postsynaptic density of excitatory synapses. Neurosci. Res. *60*, 199–212.
15. Scholz, R., Berberich, S., Rathgeber, L., Kolleker, A., Köhr, G., and Kornau, H.C. (2010). AMPA receptor signaling through BRAG2 and Arf6 critical for long-term synaptic depression. Neuron *66*, 768–780.
16. Lowenthal, M.S., Markey, S.P., and Dosemeci, A. (2015). Quantitative mass spectrometry measurements reveal stoichiometry of principal postsynaptic density proteins. J. Proteome Res. *14*, 2528–2538.
17. Brown, J.C., Petersen, A., Zhong, L., Himelright, M.L., Murphy, J.A., Walikonis, R.S., and Gerges, N.Z. (2016). Bidirectional regulation of synaptic transmission by BRAG1/IQSEC2 and its requirement in long-term depression. Nat. Commun. *7*, 11080.
18. Myers, K.R., Wang, G., Sheng, Y., Conger, K.K., Casanova, J.E., and Zhu, J.J. (2012). Arf6-GEF BRAG1 regulates JNK-mediated synaptic removal of GluA1-containing AMPA receptors: a new mechanism for nonsyndromic X-linked mental disorder. J. Neurosci. *32*, 11716–11726.
19. Awasthi, A., Ramachandran, B., Ahmed, S., Benito, E., Shinoda, Y., Nitzan, N., Heukamp, A., Rannio, S., Martens, H., Barth, J., et al. (2019). Synaptotagmin-3 drives AMPA receptor endocytosis, depression of synapse strength, and forgetting. Science *363*, 363.
20. Elagabani, M.N., Brišević, D., Kintscher, M., Pohle, J., Köhr, G., Schmitz, D., and Kornau, H.C. (2016). Subunit-selective N-Methyl-d-aspartate (NMDA) Receptor Signaling through Brefeldin A-resistant Arf Guanine Nucleotide Exchange Factors BRAG1 and BRAG2 during Synapse Maturation. J. Biol. Chem. *291*, 9105–9118.
21. Shoubridge, C., Walikonis, R.S., Gécz, J., and Harvey, R.J. (2010). Subtle functional defects in the Arf-specific guanine nucleotide exchange factor IQSEC2 cause non-syndromic X-linked intellectual disability. Small GTPases *1*, 98–103.
22. Helm, B.M., Powis, Z., Prada, C.E., Casasbuenas-Alarcon, O.L., Balmakund, T., Schaefer, G.B., Kahler, S.G., Kaylor, J., Winter, S., Zarate, Y.A., and Schrier Vergano, S.A. (2017). The role of IQSEC2 in syndromic intellectual disability: Narrowing the diagnostic odyssey. Am. J. Med. Genet. A. *173*, 2814–2820.
23. Zerem, A., Haginoya, K., Lev, D., Blumkin, L., Kivity, S., Linder, I., Shoubridge, C., Palmer, E.E., Field, M., Boyle, J., et al. (2016). The molecular and phenotypic spectrum of IQSEC2-related epilepsy. Epilepsia *57*, 1858–1869.

24. Shoubridge, C., Tarpey, P.S., Abidi, F., Ramsden, S.L., Rujirabanjerd, S., Murphy, J.A., Boyle, J., Shaw, M., Gardner, A., Proos, A., et al. (2010). Mutations in the guanine nucleotide exchange factor gene IQSEC2 cause nonsyndromic intellectual disability. Nat. Genet. *42*, 486–488.
25. Barshir, R., Hekselman, I., Shemesh, N., Sharon, M., Novack, L., and Yeger-Lotem, E. (2018). Role of duplicate genes in determining the tissue-selectivity of hereditary diseases. PLoS Genet. *14*, e1007327.
26. Bashaw, G.J., and Klein, R. (2010). Signaling from axon guidance receptors. Cold Spring Harb. Perspect. Biol. *2*, a001941.
27. Rothberg, J.M., Jacobs, J.R., Goodman, C.S., and Artavanis-Tsakonas, S. (1990). slit: an extracellular protein necessary for development of midline glia and commissural axon pathways contains both EGF and LRR domains. Genes Dev. *4* (12A), 2169–2187.
28. Seeger, M., Tear, G., Ferres-Marco, D., and Goodman, C.S. (1993). Mutations affecting growth cone guidance in Drosophila: genes necessary for guidance toward or away from the midline. Neuron *10*, 409–426.
29. Kidd, T., Bland, K.S., and Goodman, C.S. (1999). Slit is the midline repellent for the robo receptor in Drosophila. Cell *96*, 785–794.
30. Brose, K., Bland, K.S., Wang, K.H., Arnott, D., Henzel, W., Goodman, C.S., Tessier-Lavigne, M., and Kidd, T. (1999). Slit proteins bind Robo receptors and have an evolutionarily conserved role in repulsive axon guidance. Cell *96*, 795–806.
31. Tear, G., Harris, R., Sutaria, S., Kilomanski, K., Goodman, C.S., and Seeger, M.A. (1996). commissureless controls growth cone guidance across the CNS midline in Drosophila and encodes a novel membrane protein. Neuron *16*, 501–514.
32. Keleman, K., Rajagopalan, S., Cleppien, D., Teis, D., Paiha, K., Huber, L.A., Technau, G.M., and Dickson, B.J. (2002). Comm sorts robo to control axon guidance at the Drosophila midline. Cell *110*, 415–427.
33. Unni, D.K., Piper, M., Moldrich, R.X., Gobius, I., Liu, S., Fothergill, T., Donahoo, A.L., Baisden, J.M., Cooper, H.M., and Richards, L.J. (2012). Multiple Slits regulate the development of midline glial populations and the corpus callosum. Dev. Biol. *365*, 36–49.
34. Li, H., and Durbin, R. (2009). Fast and accurate short read alignment with Burrows-Wheeler transform. Bioinformatics *25*, 1754–1760.
35. DePristo, M.A., Banks, E., Poplin, R., Garimella, K.V., Maguire, J.R., Hartl, C., Philippakis, A.A., del Angel, G., Rivas, M.A., Hanna, M., et al. (2011). A framework for variation discovery and genotyping using next-generation DNA sequencing data. Nat. Genet. *43*, 491–498.
36. Pruitt, K.D., Tatusova, T., and Maglott, D.R. (2007). NCBI reference sequences (RefSeq): a curated non-redundant sequence database of genomes, transcripts and proteins. Nucleic Acids Res. *35*, D61–D65.
37. Makrythanasis, P., Nelis, M., Santoni, F.A., Guipponi, M., Vannier, A., Béna, F., Gimelli, S., Stathaki, E., Temtamy, S., Mégarbané, A., et al. (2014). Diagnostic exome sequencing to elucidate the genetic basis of likely recessive disorders in consanguineous families. Hum. Mutat. *35*, 1203–1210.
38. Ansar, M., Chung, H., Waryah, Y.M., Makrythanasis, P., Falconnet, E., Rao, A.R., Guipponi, M., Narsani, A.K., Fingerhut, R., Santoni, F.A., et al. (2018). Visual impairment and progressive phthisis bulbi caused by recessive pathogenic variant in MARK3. Hum. Mol. Genet. *27*, 2703–2711.
39. Ansar, M., Riazuddin, S., Sarwar, M.T., Makrythanasis, P., Paracha, S.A., Iqbal, Z., Khan, J., Assir, M.Z., Hussain, M., Razzaq, A., et al. (2018). Biallelic variants in LINGO1 are associated with autosomal recessive intellectual disability, microcephaly, speech and motor delay. Genet. Med. *20*, 778–784.
40. Purcell, S., Neale, B., Todd-Brown, K., Thomas, L., Ferreira, M.A., Bender, D., Maller, J., Sklar, P., de Bakker, P.I., Daly, M.J., and Sham, P.C. (2007). PLINK: a tool set for whole-genome association and population-based linkage analyses. Am. J. Hum. Genet. *81*, 559–575.
41. Santoni, F.A., Makrythanasis, P., and Antonarakis, S.E. (2015). CATCHing putative causative variants in consanguineous families. BMC Bioinformatics *16*, 310.
42. Ansar, M., Ullah, F., Paracha, S.A., Adams, D.J., Lai, A., Pais, L., Iwaszkiewicz, J., Millan, F., Sarwar, M.T., Agha, Z., et al. (2019). Bi-allelic Variants in DYNC1I2 Cause Syndromic Microcephaly with Intellectual Disability, Cerebral Malformations, and Dysmorphic Facial Features. Am. J. Hum. Genet. *104*, 1073–1087.
43. Neveling, K., Feenstra, I., Gilissen, C., Hoefsloot, L.H., Kamsteeg, E.J., Mensenkamp, A.R., Rodenburg, R.J., Yntema, H.G., Spruijt, L., Vermeer, S., et al. (2013). A post-hoc comparison of the utility of sanger sequencing and exome sequencing for the diagnosis of heterogeneous diseases. Hum. Mutat. *34*, 1721–1726.
44. Nagarkar-Jaiswal, S., DeLuca, S.Z., Lee, P.T., Lin, W.W., Pan, H., Zuo, Z., Lv, J., Spradling, A.C., and Bellen, H.J. (2015). A genetic toolkit for tagging intronic MiMIC containing genes. eLife *4*, e08469.
45. Nagarkar-Jaiswal, S., Lee, P.T., Campbell, M.E., Chen, K., Anguiano-Zarate, S., Gutierrez, M.C., Busby, T., Lin, W.W., He, Y., Schulze, K.L., et al. (2015). A library of MiMICs allows tagging of genes and reversible, spatial and temporal knockdown of proteins in Drosophila. eLife *4*, e05338.
46. Ito, K., Awano, W., Suzuki, K., Hiromi, Y., and Yamamoto, D. (1997). The Drosophila mushroom body is a quadruple structure of clonal units each of which contains a virtually identical set of neurones and glial cells. Development *124*, 761–771.
47. Luo, L., Liao, Y.J., Jan, L.Y., and Jan, Y.N. (1994). Distinct morphogenetic functions of similar small GTPases: Drosophila Drac1 is involved in axonal outgrowth and myoblast fusion. Genes Dev. *8*, 1787–1802.
48. Ni, J.Q., Zhou, R., Czech, B., Liu, L.P., Holderbaum, L., Yang-Zhou, D., Shim, H.S., Tao, R., Handler, D., Karpowicz, P., et al. (2011). A genome-scale shRNA resource for transgenic RNAi in Drosophila. Nat. Methods *8*, 405–407.
49. Dietzl, G., Chen, D., Schnorrer, F., Su, K.C., Barinova, Y., Fellner, M., Gasser, B., Kinsey, K., Oppel, S., Scheiblauer, S., et al. (2007). A genome-wide transgenic RNAi library for conditional gene inactivation in Drosophila. Nature *448*, 151–156.
50. Marcogliese, P.C., Shashi, V., Spillmann, R.C., Stong, N., Rosenfeld, J.A., Koenig, M.K., Martínez-Agosto, J.A., Herzog, M., Chen, A.H., Dickson, P.I., et al.; Program for Undiagnosed Diseases (UD-PrOZA); and Undiagnosed Diseases Network (2018). IRF2BPL Is Associated with Neurological Phenotypes. Am. J. Hum. Genet. *103*, 456.
51. Bischof, J., Björklund, M., Furger, E., Schertel, C., Taipale, J., and Basler, K. (2013). A versatile platform for creating a comprehensive UAS-ORFeome library in Drosophila. Development *140*, 2434–2442.
52. Venken, K.J., He, Y., Hoskins, R.A., and Bellen, H.J. (2006). P[acman]: a BAC transgenic platform for targeted insertion of large DNA fragments in D. melanogaster. Science *314*, 1747–1751.

53. Müller, H.A. (2008). Immunolabeling of embryos. Methods Mol. Biol. *420*, 207–218.
54. Verstreken, P., Koh, T.W., Schulze, K.L., Zhai, R.G., Hiesinger, P.R., Zhou, Y., Mehta, S.Q., Cao, Y., Roos, J., and Bellen, H.J. (2003). Synaptojanin is recruited by endophilin to promote synaptic vesicle uncoating. Neuron *40*, 733–748.
55. Goebbels, S., Bormuth, I., Bode, U., Hermanson, O., Schwab, M.H., and Nave, K.A. (2006). Genetic targeting of principal neurons in neocortex and hippocampus of NEX-Cre mice. Genesis *44*, 611–621.
56. Mazzoni, F., Novelli, E., and Strettoi, E. (2008). Retinal ganglion cells survive and maintain normal dendritic morphology in a mouse model of inherited photoreceptor degeneration. J. Neurosci. *28*, 14282–14292.
57. Lek, M., Karczewski, K.J., Minikel, E.V., Samocha, K.E., Banks, E., Fennell, T., O'Donnell-Luria, A.H., Ware, J.S., Hill, A.J., Cummings, B.B., et al.; Exome Aggregation Consortium (2016). Analysis of protein-coding genetic variation in 60,706 humans. Nature *536*, 285–291.
58. Davydov, E.V., Goode, D.L., Sirota, M., Cooper, G.M., Sidow, A., and Batzoglou, S. (2010). Identifying a high fraction of the human genome to be under selective constraint using GERP++. PLoS Comput. Biol. *6*, e1001025.
59. Kumar, P., Henikoff, S., and Ng, P.C. (2009). Predicting the effects of coding non-synonymous variants on protein function using the SIFT algorithm. Nat. Protoc. *4*, 1073–1081.
60. Adzhubei, I.A., Schmidt, S., Peshkin, L., Ramensky, V.E., Gerasimova, A., Bork, P., Kondrashov, A.S., and Sunyaev, S.R. (2010). A method and server for predicting damaging missense mutations. Nat. Methods *7*, 248–249.
61. Schwarz, J.M., Rödelsperger, C., Schuelke, M., and Seelow, D. (2010). MutationTaster evaluates disease-causing potential of sequence alterations. Nat. Methods *7*, 575–576.
62. Sobreira, N., Schiettecatte, F., Valle, D., and Hamosh, A. (2015). GeneMatcher: a matching tool for connecting investigators with an interest in the same gene. Hum. Mutat. *36*, 928–930.
63. Hu, Y., Flockhart, I., Vinayagam, A., Bergwitz, C., Berger, B., Perrimon, N., and Mohr, S.E. (2011). An integrative approach to ortholog prediction for disease-focused and other functional studies. BMC Bioinformatics *12*, 357.
64. Wang, J., Mao, D., Fazal, F., Kim, S.Y., Yamamoto, S., Bellen, H., and Liu, Z. (2019). Using MARRVEL v1.2 for Bioinformatics Analysis of Human Genes and Variant Pathogenicity. Curr. Protoc. Bioinformatics *67*, e85.
65. Venken, K.J., Schulze, K.L., Haelterman, N.A., Pan, H., He, Y., Evans-Holm, M., Carlson, J.W., Levis, R.W., Spradling, A.C., Hoskins, R.A., and Bellen, H.J. (2011). MiMIC: a highly versatile transposon insertion resource for engineering Drosophila melanogaster genes. Nat. Methods *8*, 737–743.
66. Sakagami, H., Katsumata, O., Hara, Y., Tamaki, H., Watanabe, M., Harvey, R.J., and Fukaya, M. (2013). Distinct synaptic localization patterns of brefeldin A-resistant guanine nucleotide exchange factors BRAG2 and BRAG3 in the mouse retina. J. Comp. Neurol. *521*, 860–876.
67. Katsumata, O., Ohara, N., Tamaki, H., Niimura, T., Naganuma, H., Watanabe, M., and Sakagami, H. (2009). IQ-ArfGEF/BRAG1 is associated with synaptic ribbons in the mouse retina. Eur. J. Neurosci. *30*, 1509–1516.
68. Gray, E.G. (1959). Electron microscopy of synaptic contacts on dendrite spines of the cerebral cortex. Nature *183*, 1592–1593.
69. Harris, K.M., and Kater, S.B. (1994). Dendritic spines: cellular specializations imparting both stability and flexibility to synaptic function. Annu. Rev. Neurosci. *17*, 341–371.
70. Yuste, R. (2013). Electrical compartmentalization in dendritic spines. Annu. Rev. Neurosci. *36*, 429–449.
71. Purpura, D.P. (1974). Dendritic spine "dysgenesis" and mental retardation. Science *186*, 1126–1128.
72. Phillips, M., and Pozzo-Miller, L. (2015). Dendritic spine dysgenesis in autism related disorders. Neurosci. Lett. *601*, 30–40.
73. Feng, G., Mellor, R.H., Bernstein, M., Keller-Peck, C., Nguyen, Q.T., Wallace, M., Nerbonne, J.M., Lichtman, J.W., and Sanes, J.R. (2000). Imaging neuronal subsets in transgenic mice expressing multiple spectral variants of GFP. Neuron *28*, 41–51.
74. Kalscheuer, V.M., James, V.M., Himelright, M.L., Long, P., Oegema, R., Jensen, C., Bienek, M., Hu, H., Haas, S.A., Topf, M., et al. (2016). Novel Missense Mutation A789V in IQSEC2 Underlies X-Linked Intellectual Disability in the MRX78 Family. Front. Mol. Neurosci. *8*, 85.
75. Tran Mau-Them, F., Willems, M., Albrecht, B., Sanchez, E., Puechberty, J., Endele, S., Schneider, A., Ruiz Pallares, N., Missirian, C., Rivier, F., et al. (2014). Expanding the phenotype of IQSEC2 mutations: truncating mutations in severe intellectual disability. Eur. J. Hum. Genet. *22*, 289–292.
76. Shoubridge, C., Harvey, R.J., and Dudding-Byth, T. (2019). IQSEC2 mutation update and review of the female-specific phenotype spectrum including intellectual disability and epilepsy. Hum. Mutat. *40*, 5–24.
77. Gandomi, S.K., Farwell Gonzalez, K.D., Parra, M., Shahmirzadi, L., Mancuso, J., Pichurin, P., Temme, R., Dugan, S., Zeng, W., and Tang, S. (2014). Diagnostic exome sequencing identifies two novel IQSEC2 mutations associated with X-linked intellectual disability with seizures: implications for genetic counseling and clinical diagnosis. J. Genet. Couns. *23*, 289–298.
78. Gilissen, C., Hehir-Kwa, J.Y., Thung, D.T., van de Vorst, M., van Bon, B.W., Willemsen, M.H., Kwint, M., Janssen, I.M., Hoischen, A., Schenck, A., et al. (2014). Genome sequencing identifies major causes of severe intellectual disability. Nature *511*, 344–347.
79. Rauch, A., Wieczorek, D., Graf, E., Wieland, T., Endele, S., Schwarzmayr, T., Albrecht, B., Bartholdi, D., Beygo, J., Di Donato, N., et al. (2012). Range of genetic mutations associated with severe non-syndromic sporadic intellectual disability: an exome sequencing study. Lancet *380*, 1674–1682.
80. Monies, D., Abouelhoda, M., Assoum, M., Moghrabi, N., Rafiullah, R., Almontashiri, N., Alowain, M., Alzaidan, H., Alsayed, M., Subhani, S., et al. (2019). Lessons Learned from Large-Scale, First-Tier Clinical Exome Sequencing in a Highly Consanguineous Population. Am. J. Hum. Genet. *104*, 1182–1201.
81. Yamamoto, S., Jaiswal, M., Charng, W.L., Gambin, T., Karaca, E., Mirzaa, G., Wiszniewski, W., Sandoval, H., Haelterman, N.A., Xiong, B., et al. (2014). A drosophila genetic resource of mutants to study mechanisms underlying human genetic diseases. Cell *159*, 200–214.
82. Hamosh, A., Scott, A.F., Amberger, J.S., Bocchini, C.A., and McKusick, V.A. (2005). Online Mendelian Inheritance in Man (OMIM), a knowledgebase of human genes and genetic disorders. Nucleic Acids Res. *33*, D514–D517.
83. Bellen, H.J., Wangler, M.F., and Yamamoto, S. (2019). The fruit fly at the interface of diagnosis and pathogenic mechanisms

of rare and common human diseases. Hum. Mol. Genet., ddz135.

84. Hinze, S.J., Jackson, M.R., Lie, S., Jolly, L., Field, M., Barry, S.C., Harvey, R.J., and Shoubridge, C. (2017). Incorrect dosage of IQSEC2, a known intellectual disability and epilepsy gene, disrupts dendritic spine morphogenesis. Transl. Psychiatry *7*, e1110.
85. Kinoshita-Kawada, M., Hasegawa, H., Hongu, T., Yanagi, S., Kanaho, Y., Masai, I., Mishima, T., Chen, X., Tsuboi, Y., Rao, Y., et al. (2019). A crucial role for Arf6 in the response of commissural axons to Slit. Development *146*, 146.
86. Pajcini, K.V., Pomerantz, J.H., Alkan, O., Doyonnas, R., and Blau, H.M. (2008). Myoblasts and macrophages share molecular components that contribute to cell-cell fusion. J. Cell Biol. *180*, 1005–1019.
87. Laumonnier, F., Bonnet-Brilhault, F., Gomot, M., Blanc, R., David, A., Moizard, M.P., Raynaud, M., Ronce, N., Lemonnier, E., Calvas, P., et al. (2004). X-linked mental retardation and autism are associated with a mutation in the NLGN4 gene, a member of the neuroligin family. Am. J. Hum. Genet. *74*, 552–557.
88. Massey, P.V., and Bashir, Z.I. (2007). Long-term depression: multiple forms and implications for brain function. Trends Neurosci. *30*, 176–184.
89. Kessels, H.W., and Malinow, R. (2009). Synaptic AMPA receptor plasticity and behavior. Neuron *61*, 340–350.
90. Choi, S., Ko, J., Lee, J.R., Lee, H.W., Kim, K., Chung, H.S., Kim, H., and Kim, E. (2006). ARF6 and EFA6A regulate the development and maintenance of dendritic spines. J. Neurosci. *26*, 4811–4819.
91. Kim, Y., Lee, S.E., Park, J., Kim, M., Lee, B., Hwang, D., and Chang, S. (2015). ADP-ribosylation factor 6 (ARF6) bidirectionally regulates dendritic spine formation depending on neuronal maturation and activity. J. Biol. Chem. *290*, 7323–7335.